THE ASTRONOMICAL JOURNAL, 121:1551–1555, 2001 March

HERBIG-HARO OBJECTS HH 434–436: PART OF A GIANT FLOW DRIVEN BY THE CENTRAL SOURCE A/B OF IRAS 04325+2402?

HONGCHI WANG,[1,2] JI YANG,[1,2] MIN WANG,[1,2] LICAI DENG,[2,3,4] JUN YAN,[1,2] AND JIANSHENG CHEN[2,3,4]

Received 2000 October 17; accepted 2000 December 11

ABSTRACT

While carrying out a wide-field survey of nearby star-forming regions for Herbig-Haro (HH) objects we discovered three Herbig-Haro objects, HH 434–436, in a $\sim 2' \times 2'$ (0.08 × 0.08 pc) region near L1536. HH 434 consists of three knots. HH 435 shows a bow shock shape, and HH 436 is an elongated patch. Spectroscopic observations indicate that the excitation levels of HH 434–436 are different: HH 436 has a high excitation level, while 434A has an intermediate, and 435 has a low excitation level. The overall morphology of HH 434–436 shows a bow shock shape and suggests that HH 434–436 may be a single bow shock fragmented into separate knots. Near-infrared observations of the region in the JHK' broad bands and H_2 $v = 1$–0 $S(1)$ narrow band were also carried out, but no embedded source was detected. The overall bow shock of HH 434–436 points back toward an embedded multiple system, IRAS 04325+2402. Moreover, from *Hubble Space Telescope* Near Infrared Camera and Multi-Object Spectrometer 3 observations HH 434–436 are located on the expected outflow axis of the central source A/B of this multiple system. On the basis of these facts we propose that HH 434–436 may be driven by the central source A/B of IRAS 04325+2402; therefore, they are probably part of a giant HH flow, which has a scale of 2.4 pc, although the possibility that HH 434–436 are three distinct flows cannot be completely ruled out.

Key words: ISM: Herbig-Haro objects — ISM: jets and outflows — stars: formation — stars: pre–main-sequence

1. INTRODUCTION

Protostars produce mass outflows along their polar axes while they are still accreting mass from the disks and envelopes that surround them. Herbig-Haro objects are small-scale shock regions intimately associated with star-forming regions.[5] Although mass outflows from young stellar objects (YSOs) have their demonstrations in the near-infrared and millimeter-wave bands such as molecular hydrogen emissions (e.g., McCaughrean, Rayner, & Zinnecker 1994) and CO outflows (e.g., Gueth & Guilloteau 1999), Herbig-Haro phenomena provide unique insights into the processes that lead to the formation of stars (Reipurth & Heathcote 1997). Particularly in the past few years more than two dozen parsec-scale giant HH flows have been found in the nearby star-forming regions (Bally & Devine 1994; Reipurth, Bally, & Devine 1997). These flows are up to 10 times longer than previously recognized HH flows and imply that mass loss from YSOs may profoundly affect the molecular cloud environment in active star formation regions and may play an important role in cloud dynamics.

We have carried out a wide-field survey of star-forming regions for Herbig-Haro objects to investigate the outflow activity of these regions (Yan et al. 1998; Zhao et al. 1999; Wang et al. 2000; Yang & Yao 2000). The HH objects discovered in our survey display various morphologies, such as knots, patches, bow shocks, jets, and complex structures. In this paper we report our discovery of three HH objects, HH 434–436, in the region near the dark cloud L1536. Low-dispersion spectroscopic observations were made toward HH 434A, 435, and 436. Near-infrared JHK' broadband and H_2 $v = 1$–0 $S(1)$ narrowband imaging was also made to search for embedded sources and associated H_2 emissions. Finally, a survey of nearby YSOs in the literature is made to identify the possible exciting sources of HH 434–436.

2. OBSERVATIONS AND DATA REDUCTION

The optical imaging was carried out at Xinglong Station of Beijing Astronomical Observatory (BAO). The telescope used is the f/3 60/90 cm Schmidt telescope equipped with a 2048 × 2048 Aerospace Ford CCD, which has a field of view of $57' \times 57'$. The pixel size is 15 μm, corresponding to a resolution of $1''.67$ pixel^{-1} (Fan et al. 1996). The discovery of HH 434–436 was made in our quick survey of HH objects on 1995 November 15 using two BATC[6] intermediate-band filters, [BATC09] ($\lambda_c = 6660$ Å, $\Delta\lambda = 480$ Å) and [BATC10] ($\lambda_c = 7050$ Å, $\Delta\lambda = 300$ Å) and was subsequently confirmed by narrowband [S II] filter ($\lambda_c = 6725$ Å, $\Delta\lambda = 50$ Å) observations on 1996 December 6. The [BATC09] filter well covers the strong and characteristic lines of HH objects, while the [BATC10] band covers no strong line of HH objects and therefore is used to measure the continuum. Three frames in each band of [BATC09], [BATC10], and [S II] were taken so that the cosmic rays and the bad pixels could be removed. The total exposures in [BATC09], [BATC10], and [S II] bands are 1440, 1440, and 3600 s, respectively. The seeing during the observations was typically $\sim 2''$. Bias subtraction, dome flat-field normalization, and image combination were conducted using the IRAF package.

[1] Purple Mountain Observatory, Academia Sinica, Nanjing, Jiangsu, 210008, China.
[2] Chinese National Astronomical Observatories, Chinese Academy of Sciences, A20 Datun Road, Chaoyang District, Beijing 100012, China.
[3] Beijing Astronomical Observatory, Chinese Academy of Sciences, Beijing 100012, China.
[4] Beijing Astrophysical Center, Chinese Academy of Sciences and Peking University, Beijing 100012, China.
[5] See http://casa.colorado.edu/hhcat.

[6] BATC: Beijing Arizona Taiwan Connecticut Multicolor Sky Survey.

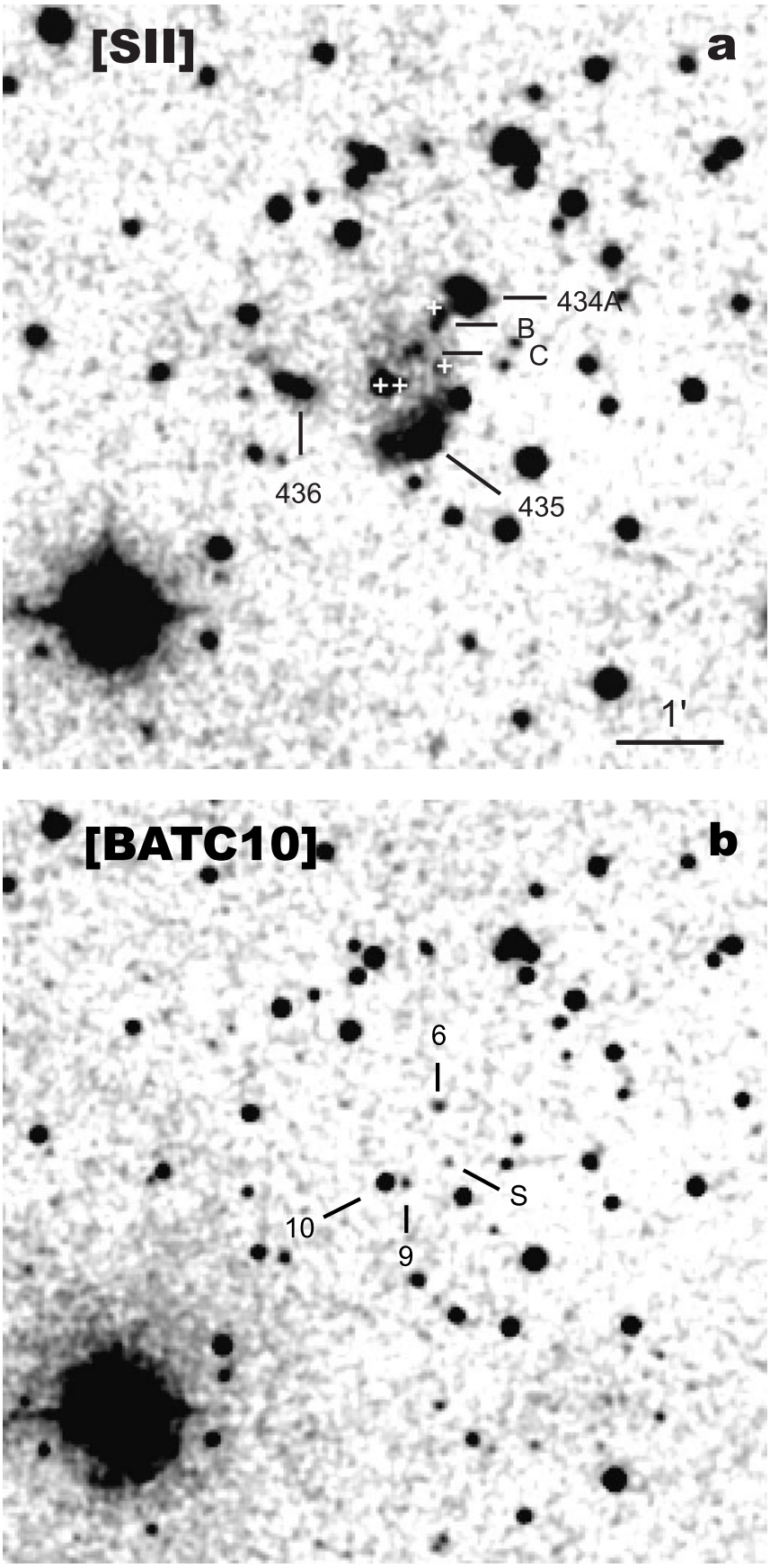

FIG. 1.—Images of HH 434–436 in (*a*) [S II] band and (b) [BATC10] band. Stars 6, 9, 10, and S from Table 2 are marked with plus signs in (*a*) and labeled in (*b*). All the fields are 7′ × 7′. North is up, east is to the left, and the scale is shown in (*a*).

Low-dispersion spectroscopic observations of HH 434A, 435, and 436 were made with the BAO 2.16 m reflector using a Cassegrain spectrograph during the period 1999 December 4–9. The grating used is 100 Å mm^{-1}, and the slit width is 1.″5. The resulting spectral resolution is ~ 7 Å.

The near-infrared observations were carried out on 1999 November 18 at the 1.88 m telescope in Okayama Astronomical Observatory, Japan, using the infrared camera OASIS (Yamashita et al. 1995). OASIS, equipped with a near-infrared camera and multiobject spectrometer array (NICMOS3), provides a field of view of 4.′2 × 4.′2 with a resolution of 0.″97 $pixel^{-1}$. Five dithered J, H, K' (2.16 μm) and H_2 $v = 1$–0 $S(1)$ (2.12 μm) images were obtained, and the total exposures were 150, 50, 50, and 300 s, respectively. The weather conditions during the observations were good, and the seeing was around 2.″0. The images were dark-subtracted, flat field–normalized, sky frame–subtracted, registered, and combined using the IRAF package. The flat field was constructed with two sets of dome flat frames taken by switching an illuminating lamp on and off. The sky frame was obtained by median filtering the target images. The standard stars used are AS 08-0 and AS 08-2 (Hunt et al. 1998). The estimated uncertainties in our photometry are typically 0.1 mag. The 5 σ limiting magnitudes for the J, H, K' bands are 20.5, 18.8, and 18.3 mag $pixel^{-1}$, respectively.

3. RESULTS AND DISCUSSION

In Figure 1 we present the images of the newly found HH objects, HH 434–436, in [S II] and [BATC10] bands. The details of HH 434–436 could be seen more clearly in the contour map of the region (Fig. 2). The HH nature of HH 434–436 is apparent from the [S II] and [BATC10] images. The coordinates of HH 434–436 in the 1950 epoch are listed in Table 1. The astrometry is done by using the Guide Star Catalog (GSC).

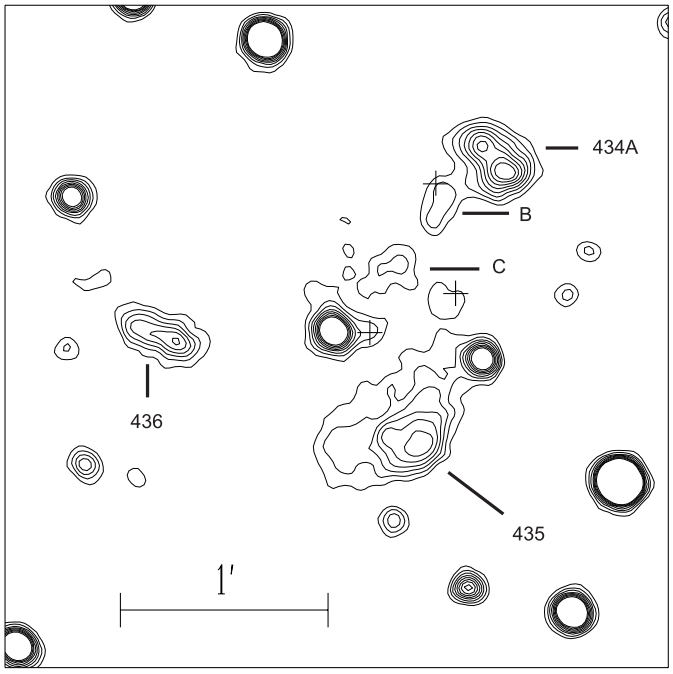

FIG. 2.—Contour map of the HH 434–436 region. The lowest level corresponds to 3 σ (the sky noise level), and the interval is 2 σ. Stars 6, 9, and S from Table 2 are marked with plus signs.

TABLE 1

NEW HERBIG-HARO OBJECTS

Object	α (1950)	δ (1950)	Comments
HH 434A.....	4 31 12.99	23 03 16.2	Knot
HH 434B.....	4 31 14.22	23 03 09.4	Knot
HH 434C.....	4 31 15.26	23 02 47.1	Knot
HH 435.....	4 31 14.90	23 01 55.7	Bow shock
HH 436.....	4 31 20.15	23 02 28.0	Elongated patch

NOTE.—Units of right ascension are hours, minutes, and seconds, and units of declination are degrees, arcminutes, and arcseconds.

HH 434 consists of three knots, 434A–C. From Figure 2 we could see that the 434A knot consists of two condensations. HH 435 is a bright bow shock with its axis of symmetry in the direction of P.A. $\simeq 25°$. HH 436 is a bright patch elongated in the direction of P.A. $\simeq 65°$. A faint patch of [S II] emission can be identified northeast of HH 436. Moreover, there is diffuse [S II] emission around stars 9, 10, and S.

The low-dispersion spectra of HH 434–436 are shown in Figure 3. For spectroscopic observations the total exposures for HH 434A, 435, and 436 are 90, 90, and 180 minutes, respectively. The slit positions are all centered on the [S II] emission maximums and are oriented along the north-south direction. The spatial extents where the spectra are extracted are 23″, 16″, and 10″ for HH 434A, 435, and 436, respectively. From the spectra we obtained the following line intensity ratios: [O I] $\lambda\lambda(6300 + 6363)/H\alpha \approx 0.40$,

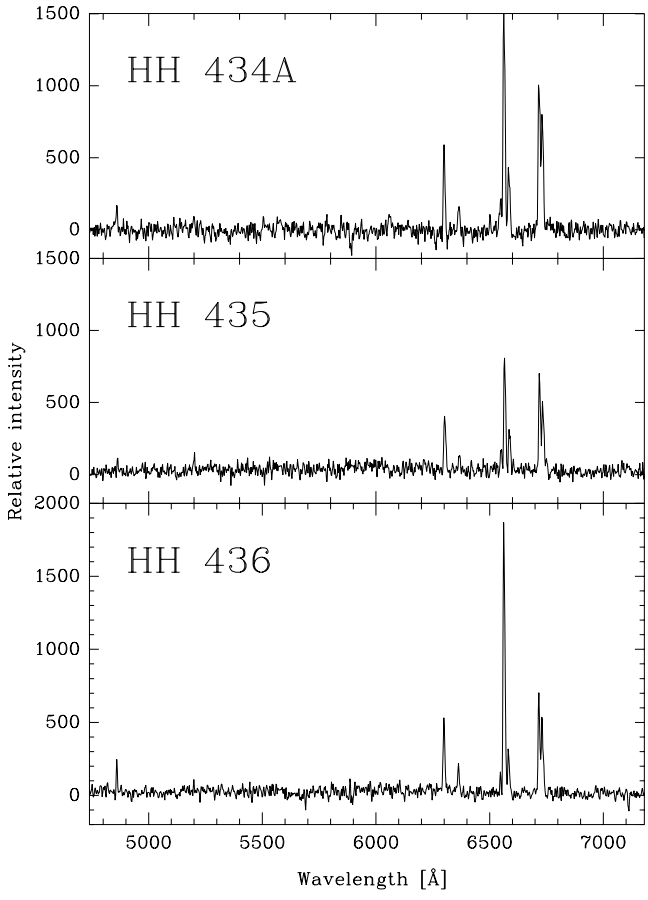

FIG. 3.—Low-dispersion spectra of HH 434–436

[N II] $\lambda\lambda(6548 + 6583)/H\alpha \approx 0.41$, [S II] $\lambda\lambda(6717 + 6731)/H\alpha \approx 1.12$ for HH 434A; [O I] $\lambda\lambda(6300 + 6363)/H\alpha \approx 0.64$, [N II] $\lambda\lambda(6548 + 6583)/H\alpha \approx 0.50$, [S II] $\lambda\lambda(6717 + 6731)/H\alpha \approx 1.41$ for HH 435; and [O I] $\lambda\lambda(6300 + 6363)/H\alpha \approx 0.37$, [N II] $\lambda\lambda(6548 + 6583)/H\alpha \approx 0.22$, [S II] $\lambda\lambda(6717 + 6731)/H\alpha \approx 0.61$ for HH 436. These ratios indicate that the excitation degree of HH 435 is low while that of HH 436 is high and that of HH 434A is intermediate. The [S II] $\lambda 6717/\lambda 6731$ intensity ratios for HH 434A, 435, and 436 are 1.34, 1.43, and 1.21, respectively, which indicate an electron density of ≈ 100, 30, and 300 cm^{-3}, respectively (Osterbrock 1989).

We note that the [S II] emission structure of the HH 434–436 region displays a bow shock morphology: HH 435 shows as the head and HH 434A and 436 show as the wings of the bow shock. Therefore, although HH 434–436 have different levels of excitation, it is likely that HH 434–436 are a single bow shock rather than three distinct flows. Similar cases of different excitations within one bow shock were found in HH 2 (Torrelles et al. 1992; Schwartz et al. 1993; Hester, Stapelfeldt, & Scowen 1998) and HH 43 (Böhm & Solf 1990).

To search for associated infrared H_2 emissions and nearby embedded sources we conducted H_2 $v = 1$–0 $S(1)$ narrowband and JHK' broadband imaging of the region. The results show that no H_2 emission is detected in our H_2 image. In the K' image 18 stars are detected in the central $4'.4 \times 2'.9$ region. Their JHK' photometry is listed in Table 2. The average $J-H$ and $H-K'$ colors of these stars are 0.65 and 0.16 mag, respectively. Star 6 shows the largest $J-H$ and $H-K'$ colors, 0.88 and 0.5 mag, respectively, which, however, are located within the interstellar reddening regime in the near-infrared color-color diagram (Bessell & Brett 1988). From the JHK' photometry, therefore, we could see that there is no embedded source in the region.

The HH 434–436 region is located in the southeastern part of the Taurus complex, about 28′ northeast of the NH_3 peak of L1536 (Myers & Benson 1983) (see Fig. 4; HH objects are from Reipurth's general catalog[5]). ^{13}CO observations by Mizuno et al. (1995) indicate that there is no dense gas in the region, which is consistent with the high density of field stars of the region within the [BATC10] and [S II] images, as well as the low extinction suggested by the JHK' photometry. These facts suggest that HH 434–436 are probably not excited by nearby sources.

From Figure 4 it could be seen that the dense gas in the region is distributed along two ^{13}CO ridges and that all HH objects are located in the ^{13}CO clumps except for HH 300, 410, and 434–436. HH 300 is the southwestern bow shock of a giant flow emanating from the embedded source IRAS 04239+2436 (Reipurth et al. 1997). HH 410 belongs to a giant flow driven by the infrared companion to the T Tauri primary in Haro 6-10 (Devine et al. 1999). In the southern ^{13}CO ridge there are three known CO outflows: IRAS 04295+2251, 04302+2247, 04328+2248 (HP Tau) (Moriarty-Schieven et al. 1992; Bontemps et al. 1996; Duvert et al. 2000). In the northern ridge there are six known CO outflows: IRAS 04239+2436 (Moriarty-Schieven et al. 1992), Haro 6-10 (Terebey, Vogel, & Myers 1989), IRAS 04278+2435 (ZZ Tau) (Heyer et al. 1987), TMC 2A (Wu, Huang, & He 1996), L1529 (Lichten 1982), and IRAS 04325+2402 (Heyer et al. 1987). Position angles are available for three of these CO outflows: P.A. $\approx 160°$ for IRAS 04302+2247 (Bontemps et al. 1996; Gomez, Whitney, & Kenyon 1997), P.A. $\approx 45°$ for IRAS 04328+2248 (HP Tau) (Duvert et al. 2000), and P.A. $\approx -45°$ for IRAS 04325+2402 (Heyer et al. 1987). The above position angles and the locations of HH 434–436 show that these three CO outflows have no relationship to HH 434–436.

Near-infrared imaging and polarization observations can also reveal outflow orientations. The measured position angles of the symmetry axes, θ_{neb}, and of the polarizations, θ_p, of the infrared nebulae associated with the outflow sources are $\theta_p = 146°$ for IRAS 04239+2436 (Whitney, Kenyon, & Gómez 1997), $\theta_p = 67°$ for IRAS 04295+2251

TABLE 2

NEAR-INFRARED PHOTOMETRY OF THE HH 434–436 REGION

NIRS	ΔR.A.[a] (arcsec)	ΔDecl.[a] (arcsec)	K' (mag)	$H-K'$ (mag)	$J-H$ (mag)
1.....	−90.9	−46.7	12.82	−0.02	0.49
2.....	−82.5	22.1	16.03	0.31	0.28
3.....	−75.3	8.4	14.84	0.00	0.83
4.....	−66.2	−29.3	15.77	0.11	0.87
5.....	−47.9	−9.4	14.87	0.14	0.29
6.....	−35.6	41.8	14.99	0.5	0.88
7.....	−29.3	−68.3	15.73	0.35	0.71
8.....	−18.2	−56.8	13.79	0.24	0.74
9.....	−12.5	−0.3	15.01	0.29	0.83
10.....	0.0	0.0	13.87	0.13	0.53
11.....	25.2	45.5	16.16	0.22	0.55
12.....	62.3	−59.3	15.42	0.23	0.79
13.....	64.1	−41.5	14.87	0.25	0.73
14.....	80.6	−37.7	14.01	0.12	0.81
15.....	83.0	42.0	14.61	0.00	0.41
16.....	85.7	−2.9	15.75	−0.05	0.74
17.....	138.0	10.4	14.91	0.04	0.40
18.....	145.5	6.0	16.37	−0.04	0.79

[a] Right ascension and declination offsets from star 10, for which the position ($4^h31^m16^s.62$, 23°02′28″.7), 1950.0, is determined from GSC.

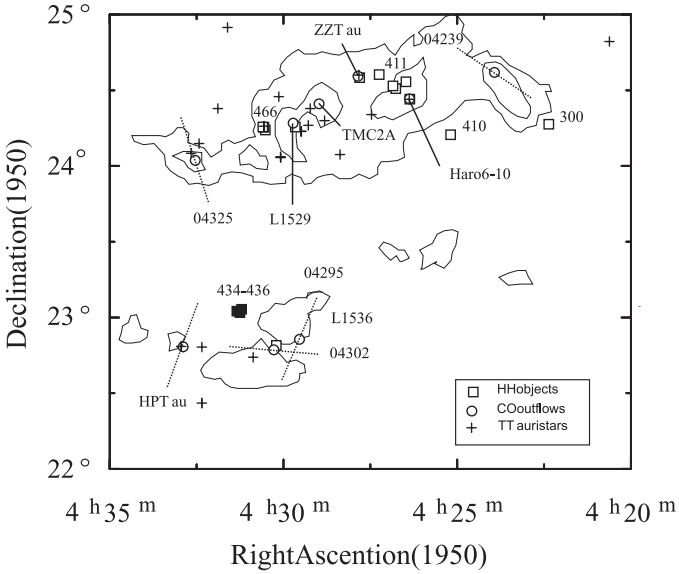

FIG. 4.—YSOs and outflows near HH 434–436, showing the outflow axes derived from infrared nebula symmetry or polarizations (*dotted lines*). The contours outline the ^{13}CO integrated intensity taken from Mizuno et al. (1995). HH objects are from Reipurth's general catalog, and T Tauri stars are from Herbig & Bell (1988).

(Whitney et al. 1997), $\theta_{neb} = 85°$ for IRAS 04302+2247 (Padgett et al. 1999), $\theta_{neb} = 18°$ for IRAS 04325+2402 (Whitney et al. 1997), and $\theta_p \approx 70°$ for each component of the IRAS 04328+2248 (HP Tau) triple system (Monin, Ménard, & Duchêne 1998). From these measurements the outflow axes can be derived by assuming that they are along the nebula symmetry axes and are perpendicular to the polarization vectors. The derived outflow axes are indicated by dotted lines in Figure 4.

IRAS 04325+2402 is in fact a multiple system. *HST*/NICMOS3 observations resolved IRAS 04325+2402 into a central source A/B and its companion, C, (Hartmann et al. 1999). Source A/B lies near the apex of the main bipolar reflection nebula, and source C is well separated from source A/B at a projected distance of 8″.2. The orientation of the main reflection nebula lies in the direction of P.A. $\approx 20°$ (see Fig. 2 of Hartmann et al. 1999). The position angle of the symmetry axis measured by Whitney et al. (1997) for the IRAS 04325+2402 infrared nebula, as illustrated in Figure 4, is consistent with the above orientation. The expected axis of an outflow from the central source A/B of IRAS 04325+2402 is along the orientation of the main reflection nebula. From Figure 4 one can see that HH 434–436 lie well on this expected outflow axis.

We note that the CO outflow at P.A. $\approx -45°$ (Heyer et al. 1987) in the IRAS 04325+2402 region is close to the orientation expected for an outflow from source C (see Fig. 7 of Hartmann et al. 1999) and completely inconsistent with the orientation of the main reflection nebula. This CO outflow should have no relationship to HH 434–436.

In summary, our *JHK′* photometry suggests that HH 434–436 are probably not excited by nearby sources. The overall bow shock of HH 434–436 shows a symmetry axis of P.A. $\approx 25°$ that points toward IRAS 04325+2402. Furthermore, HH 434–436 lie on the expected axis of an outflow from the central source A/B of IRAS 04325+2402. On the basis of these facts we suggest that HH 434–436 are probably driven by the central source A/B of IRAS 04325+2402. The angular distance between HH 434–436 and the central source A/B of IRAS 04325+2402 is 1°.0, which corresponds to a scale of 2.4 pc. Therefore, besides HH 300/300D and HH 410/411, HH 434–436 are probably another giant HH flow in the southeastern part of the Taurus complex.

We would like to thank the staff members of BATC Beijing group for helpful discussions and excellent support, the staff members of Okayama Astronomical Observatory, Japan, and the staff members of BAO for their excellent support during observations of this work. We appreciate Bo Reipurth for assigning HH numbers for our objects and also for his valuable comments. The authors are grateful to the anonymous referee for his or her valuable comments, which improved the manuscript. This research was supported by NSFC grants 19625307, 19603002, and 19803005.

REFERENCES

Bally, J., & Devine, D. 1994, ApJ, 428, L65
Bessell, M. S., & Brett, J. M. 1988, PASP, 100, 1134
Böhm, K. H., & Solf, J. 1990, ApJ, 348, 297
Bontemps, S., André, P., Terebey, S., & Cabrit, S. 1996, A&A, 311, 858
Devine, D., Reipurth, B., Bally, J., & Balonek, T. J. 1999, AJ, 117, 2931
Duvert, G., Guilloteau, S., Ménard, F., Simon, M., & Dutrey, A. 2000, A&A, 355, 165
Fan, X., et al. 1996, AJ, 112, 628
Gomez, M., Whitney, B. A., & Kenyon, S. J. 1997, AJ, 114, 1138
Gueth, F., & Guilloteau, S. 1999, A&A, 343, 571
Hartmann, L., Calvet, N., Allen, L., Chen H., & Jayawardhana, R. 1999, AJ, 118, 1784
Herbig, G. H., & Bell, K. R. 1988, Lick Obs. Bull., No. 1111, 1
Hester, J. J., Stapelfeldt, K. R., & Scowen, P. A. 1998, AJ, 116, 372
Heyer, M. H., Snell, R. L., Goldsmith, P. F., & Myers, P. C. 1987, ApJ, 321, 370
Hunt, L. K., Mannucci, F., Testi, L., Migliorini, S., Stanga, R. M., Baffa, C., Lisi, F., & Vanzi L. 1998, AJ, 115, 2594
Lichten, S. M. 1982, ApJ, 255, L119
McCaughrean, M. J., Rayner, J. T., & Zinnecker, H. 1994, ApJ, 436, L189
Mizuno, A., Onishi, T., Yonekura, Y., Nagahama, T., Ogawa, H., & Fukui, Y. 1995, ApJ, 445, L161
Monin, J.-L., Ménard, F., & Duchêne, G. 1998, A&A, 339, 113
Moriarty-Schieven, G. H., Wannier, P. G., Tamura, M., & Keene, J. 1992, ApJ, 400, 260
Myers, P. C., & Benson, P. J. 1983, ApJ, 266, 309
Osterbrock, D. E. 1989, Astrophysics of Gaseous Nebulae and Active Galactic Nuclei (Mill Valley: University Science Books)
Padgett, D., Brandner, W., Stapelfeldt, K. R., Strom, S. E., Terebey, S., & Koerner, D. 1999, AJ, 117, 1490
Reipurth, B., Bally, J., & Devine, D. 1997, AJ, 114, 2708
Reipurth, B., & Heathcote, S. 1997, in IAU Symp. 182, Herbig-Haro Flows and the Birth of Low-Mass Stars, ed. B. Reipurth & C. Bertout (Dordrecht: Kluwer), 3
Schwartz, R. D., et al. 1993, AJ, 106, 740
Terebey, S., Vogel, S. N., & Myers, P. C. 1989, ApJ, 340, 472
Torrelles, J. M., Rodríguez, L. F., Cantó, J., Anglada, G., Gómez, J. F., Curiel, S., & Ho, P. T. P. 1992, ApJ, 396, L95
Wang, M., Zhao, B., Yang, J., Deng, L., & Chen, J. 2000, Chinese Phys. Lett., 17, 304
Whitney, B. A., Kenyon, S. J., & Gómez, M. 1997, ApJ, 485, 703
Wu, Y., Huang, M., & He, J. 1996, A&AS, 115, 283
Yamashita, T., et al. 1995, in Scientific and Engineering Frontiers for 8–10 m Telescopes, ed. M. Iye & T. Nishimura (Tokyo: Universal Acad.), 285
Yan, J., Wang, H., Wang, M., Deng, L., Yang, J., & Chen, J. 1998, AJ, 116, 2438
Yang, J., & Yao, Y. 2000, in IAU Symp. 197, Astrochemistry: From Molecular Clouds to Planetary Systems, ed. Y. C. Minh & E. F. van Dishoeck (San Francisco: PASP), 213
Zhao, B., Wang, M., Yang, J., Wang, H., Deng, L., Yan, J., & Chen, J. 1999, AJ, 118, 1347